

AD _____

Award Number: W81XWH-~~EJFEH~~

TITLE: ~~Öç^[[{ ^} ö Á-á p a) [^ & @ [[[* ^ Á | æ [[{ Á | Á | [• æ ^ Á ö a) & ^ Á ö ^} ^ Á @ | a] ^~~

PRINCIPAL INVESTIGATOR: ~~Öæ @ P æ ^ - á Ú @ Ö È~~

CONTRACTING ORGANIZATION: ~~Ü ç ^ ^ • É V @ Á U æ ^ Á M, ä ^ ^ • ä Á - Á ^, Á R ^ ! • ^~~
~~p ^, Á Ö i ^ } •, æ É P R Á É J E F Á~~

REPORT DATE: R | ^ Á Ö F F

TYPE OF REPORT: Annual

PREPARED FOR: U.S. Army Medical Research and Materiel Command
Fort Detrick, Maryland 21702-5012

DISTRIBUTION STATEMENT: Approved for public release; distribution unlimited

The views, opinions and/or findings contained in this report are those of the author(s) and should not be construed as an official Department of the Army position, policy or decision unless so designated by other documentation.

REPORT DOCUMENTATION PAGE

Form Approved
OMB No. 0704-0188

Public reporting burden for this collection of information is estimated to average 1 hour per response, including the time for reviewing instructions, searching existing data sources, gathering and maintaining the data needed, and completing and reviewing this collection of information. Send comments regarding this burden estimate or any other aspect of this collection of information, including suggestions for reducing this burden to Department of Defense, Washington Headquarters Services, Directorate for Information Operations and Reports (0704-0188), 1215 Jefferson Davis Highway, Suite 1204, Arlington, VA 22202-4302. Respondents should be aware that notwithstanding any other provision of law, no person shall be subject to any penalty for failing to comply with a collection of information if it does not display a currently valid OMB control number. **PLEASE DO NOT RETURN YOUR FORM TO THE ABOVE ADDRESS.**

1. REPORT DATE (DD-MM-YYYY) 01-07-2011		2. REPORT TYPE Annual	3. DATES COVERED (From - To) 1 Jul 10-30 Jun 11		
4. TITLE AND SUBTITLE Development of a Nanotechnology Platform for Prostate Cancer Gene Therapy			5a. CONTRACT NUMBER		
			5b. GRANT NUMBER W81XWH-09-1-0303		
			5c. PROGRAM ELEMENT NUMBER		
6. AUTHOR(S) Arash Hatefi, Ph.D. E-Mail: ahatefi@pharmacy.rutgers.edu			5d. PROJECT NUMBER		
			5e. TASK NUMBER		
			5f. WORK UNIT NUMBER		
7. PERFORMING ORGANIZATION NAME(S) AND ADDRESS(ES) Rutgers, The State University of New Jersey New Brunswick, NJ 08901			8. PERFORMING ORGANIZATION REPORT NUMBER		
9. SPONSORING / MONITORING AGENCY NAME(S) AND ADDRESS(ES) U.S. Army Medical Research and Materiel Command Fort Detrick, Maryland 21702-5012			10. SPONSOR/MONITOR'S ACRONYM(S)		
			11. SPONSOR/MONITOR'S REPORT NUMBER(S)		
12. DISTRIBUTION / AVAILABILITY STATEMENT Approved for Public Release; Distribution Unlimited					
13. SUPPLEMENTARY NOTES					
14. ABSTRACT The objective of this research is to design and develop a nanocarrier that is able to evade the immune system, circulate in the blood stream, find its target prostate cancer cells, and transfer therapeutic genes into prostate cancer cells efficiently. The gene carrier is composed of: a) histone H2A peptide (H2A) to condense pDNA into nano-size particles (nanocarriers), b) a PC-3 specific targeting motif (TM) to target prostate cancer cells, c) an endosome disrupting motif (EDM) to disrupt endosome membrane and facilitate escape of the cargo into the cytosol, and d) a nuclear localization signal (NLS) to actively translocate pDNA towards the nucleus of cancer cells. The gene encoding the gene delivery system was synthesized and cloned into a pET21b vector. The vector was genetically engineered and complexed with plasmid DNA (pDNA) to form stable nanoparticles with sizes below 100nm. The nanoparticles were used to deliver reporter genes (pEGFP) to target PC-3 prostate cancer cells. The results demonstrated that the gene delivery system is able to target and efficiently transfect PC-3 cancer cells with minimum cross-reactivity with normal epithelial prostate cells. Furthermore, the gene delivery system by itself did not show any detectable toxicity in the range tested (110ug/ml). An animal protocol has been prepared and approved by IACUC and DOD ACURO.					
15. SUBJECT TERMS None provided.					
16. SECURITY CLASSIFICATION OF:			17. LIMITATION OF ABSTRACT UU	18. NUMBER OF PAGES 20	19a. NAME OF RESPONSIBLE PERSON USAMRMC
a. REPORT U	b. ABSTRACT U	c. THIS PAGE U			19b. TELEPHONE NUMBER (include area code)

Table of Contents

Introduction.....	1
Body.....	1
Key Research Accomplishments.....	5
Reportable Outcomes.....	5
Conclusions.....	5
References.....	5
Appendices.....	6

Introduction

A major obstacle to improving patients' survival with advanced prostate cancer is progression of the cancer to androgen-independence. Therefore, methods such as gene therapy capable of delay or stop this progression may have a significant impact on improving patients' health. However, many challenges lie ahead for gene therapy, including improving DNA transfer efficiency to cancer cells, enhancing levels of gene expression, and overcoming immune responses. **The overall objective** of this research is to design and develop a nanocarrier that is able to evade the immune system, circulate in the blood stream, find its target prostate cancer cells, and transfer therapeutic genes into prostate cancer cells efficiently. The gene carrier is composed of: a) histone H2A peptide (H2A) to condense plasmid DNA (pDNA) into nano-size particles (nanocarriers), b) a PC-3 specific targeting motif (TM) to target prostate cancer cells, c) an endosome disrupting motif (EDM) to disrupt endosome membranes and facilitate escape of the cargo into the cytosol, and d) a nuclear localization signal (NLS) to actively translocate pDNA towards the nucleus of cancer cells. An elastin like polymer (ELP) has also been engineered in the vector structure to provide a hydrophilic shield and protect the vector/pDNA complex in the blood stream from the immune system. For simplicity, the vector will be shown as EDM-H2A-NLS- TM or namely GHT2. PC-3 prostate cancer cells are selected as target because they are highly metastatic and characterized to be CAR⁻/HER2⁻. This means that they are not a good candidate for adenoviral gene therapy or Herceptin anti-HER2 immunotherapy. Therefore, development of a targeted delivery system for this type of prostate cancer cells could be highly beneficial.

CAR: Coxsackie Adenovirus Receptor

HER2: Human Epidermal Growth Factor Receptor 2

Body

This is the second year report; therefore, below we have highlighted the studies that have been performed in Year 2 of the DOD grant. We have met all the objectives of Year 1 and our annual report for year 1 has been approved by DOD reviewers. For year 2, months 1-12, Task 1 was proposed. All the deadlines as delineated in the Statement of Work are met in time and we are progressing as planned.

Task 1- Complex the vector with pDNA (i.e, pEGFP) to form nanocarriers, evaluate and optimize the transfection efficiency *in vitro* (months 1-12).

1.1. Vector/pDNA complexes will be formed and particles will be characterized under various physicochemical conditions including pH, temperature, and salt conditions. The nanoparticles will be stabilized and optimum conditions to form nanoparticles will be identified (months 1-5).

- The mean hydrodynamic particle size and charge of vector/pDNA complexes were determined using Dynamic Light Scattering (DLS) and Laser Doppler Velocimetry (LDV) respectively. All vectors were able to complex with pDNA and formed particles with sizes below 100nm. The particle size and charge analysis for GHT2 is shown in **Fig. 1**. This method has previously been published by our group [1]. The particles demonstrated stability under various pH, temperature (up to 37oC) and salt concentrations (up to 150mM NaCl). Because the nanoparticles demonstrated stability, they were used to transfect various cell lines.

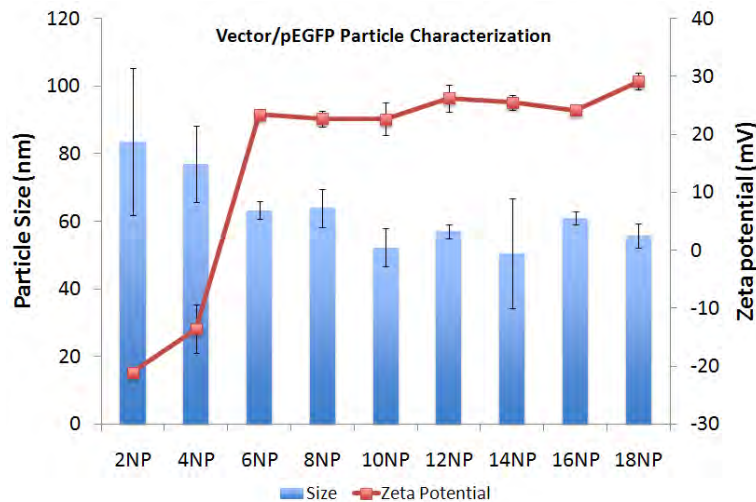


Fig. 1: Various amounts of vector in 5mM acetate buffer were added to 1 μ g of pDNA (pEGFP) to form complexes at different N:P ratios (N-atoms in vector to P-atoms in pDNA) in a total volume of 100 μ l deionized water. After 30 minutes of incubation, the size and zeta potential of the complexes were measured and reported as mean \pm SEM, (n=3). Each mean is the average of 15 measurements and n represents the number of separate batches prepared for the measurements.

1.2. Cell transfection studies will be performed using PC-3 and RWPE-2 cells. Cells will be transfected with vector/pEGFP complexes at various N/P ratios in the presence and absence of chloroquine, bafilomycin, and Nocodazole and the transfection efficiency will be measured. The cell transfection process will be optimized to obtain highest transfection efficiency (months 5-12)

- The transfection efficiency was optimized and the ability of the GHT2 vector to target and transfect PC-3 prostate cancer cells but not RWPE-1 normal epithelial prostate cells is shown in **Fig. 2**. The details of the method of cell transfection have been previously published by our group [1]. The ability of the vector to escape from endosomes and traffick pDNA towards nucleus has also been shown [1]. Please note that we had originally proposed to use RWPE-2 normal prostate epithelial cells. However, through consultation with Dr. Minko (collaborator) who has extensive experience in cancer therapy we replaced it with RWPE-1. This cell line, i.e., RWPE-1 is a more appropriate cell line and a better representative of normal human prostate cells.

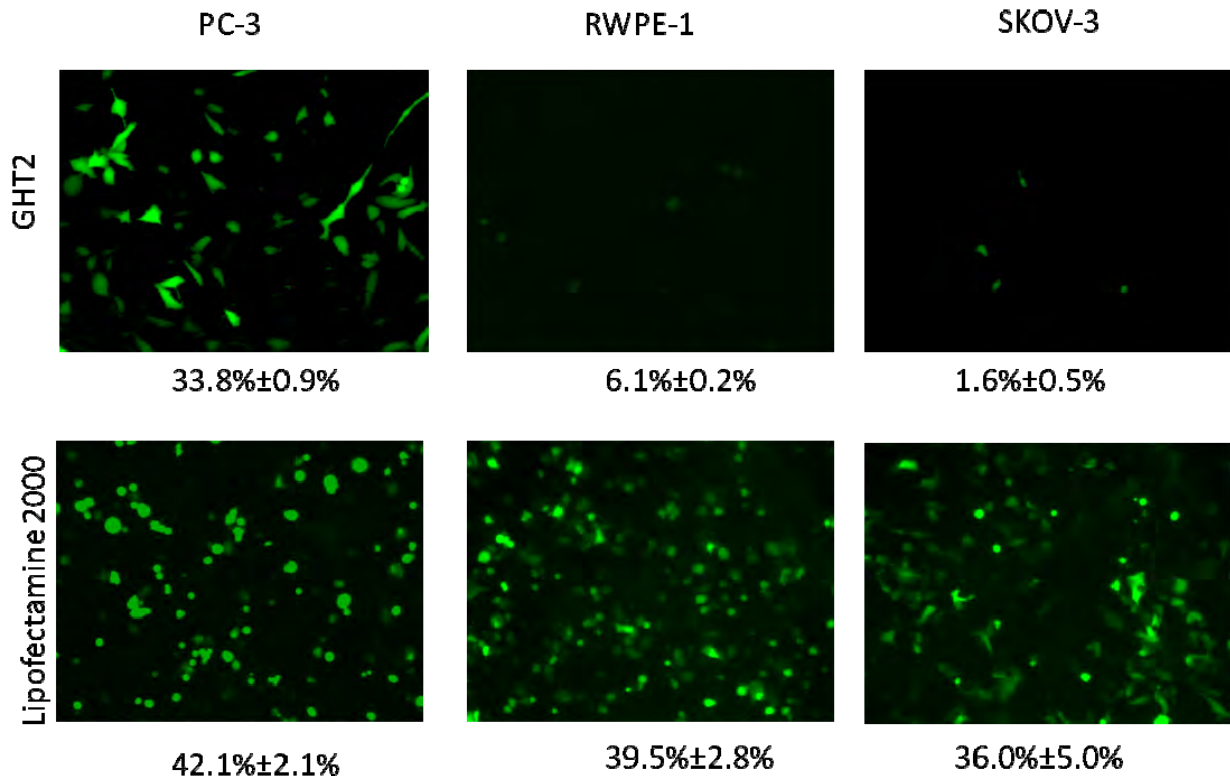


Fig. 2: Demonstration of PC-3 targeted gene delivery. Qualitative and quantitative representation of the PC-3 (CAR⁻/HER2⁻), RWPE-1 (normal cells) and SK-OV-3 cells (CAR⁺/HER2⁻) transfected with vector/pEGFP complexes at N:P ratio of 10 and lipofectamine/pEGFP. The percentage of transfected cells is measured by flowcytometer. This figure shows that the GHT2 vector can target and transfect prostate cancer cells while preserving normal cells. In contrast, commercially available vectors such as lipofectamine non-selectively transfect all cells which could result in unwanted toxicity to normal cells during the therapy.

- Using a WST-1 cell toxicity assay, the potential toxicity of the GHT2 vector to PC-3 cancer cells was evaluated. The details of this method have previously been published [1]. We did not observe any vector related toxicity in PC-3 cancer cells at any NP ratio tested (**Fig. 3**). At NP ratio of 18, 23.5µg of vector is used to complex with 1µg of pEGFP.

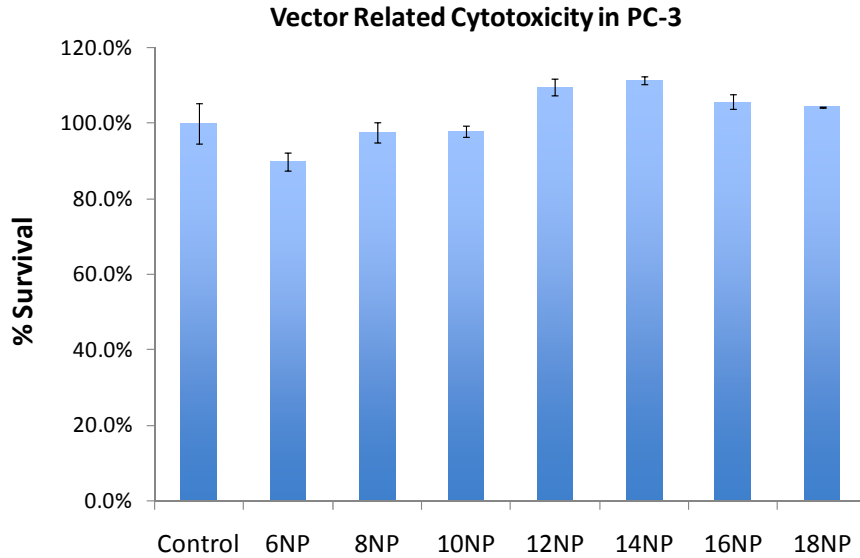


Fig. 3: PC-3 cells were seeded at 10,000 cells/well in 96-well plates. Cells were transfected with GHT2/pEGFP complexes formed at various N:P ratios (equivalent to 1 μ g pEGFP). The control group received no treatment. 48 hours after transfection, a WST-1 (Roche Applied Science, Indianapolis, IN) cytotoxicity assay was performed to determine the vector related cytotoxicity in this cell line.

1.3. An animal protocol will be prepared and submitted for approval by the IACUC (months 10-12).

- The animal protocol is prepared and approved by the IACUC (Protocol #: 10-070). The approval from DOD Animal Care and Use Review Office (ACURO) has also been obtained .

Task 2- Inject the nanocarriers in mice bearing xenograft tumor model of prostate cancer and evaluate the transfection efficiency and therapeutic efficacy (months 12-23).

2.1. To evaluate transfection efficiency, pCMV-luc or pEGFP will be complexed with vectors and used to transfect PC-3 tumors in nude mice. The transfection efficiency in tumors and other tissues will be evaluated using an in vivo imaging system. These studies will be performed using 40 nude mice (months 12-17)

- This task is in progress and has not completed yet.

Key Research Accomplishments

- a) Developed stable nanoparticles with sizes less than 100nm. This size range makes them suitable for receptor-mediated endocytosis.
- b) Formulated nanoparticles with ability to target PC-3 prostate cancer cells with high efficiency but with low binding to normal epithelial prostate cells.
- c) The engineered nanoparticles showed no acute cytotoxicity.

Reportable Outcome

A) Manuscript: In preparation

B) Presentations:

1- The PI (A. Hatefi) received an invitation from the organizers of the Nanomedicine and Drug Delivery Symposium (NanoDDS'10) to give a talk about this research. This symposium was held on October 3-5, 2010 and the work was presented.

2- The PI (A. Hatefi) also submitted an abstract (Abstract#1847) and presented this work in DoD IMPaCT 2011 conference held in Orlando, Florida.

C) Training: A Research Scientist with experience in molecular biology techniques was hired. She has received training in vector development, vector characterization, mammalian cell culture and transfection, and targeted prostate cancer gene therapy. In addition, a PhD student was trained to perform the studies. The newly recruited PhD student will be conducting the proposed animal studies under Task 2.

D) Grant application: None

E) Patent application: None

Conclusions

Using genetic engineering techniques we have created a PC-3 specific gene delivery system that can potentially be used in the treatment of the patients that do not respond to adenoviral gene therapy or Herceptin immunotherapy. The *in vivo* studies in nude mice are designed and will be performed at Rutgers University.

References

[1]- Y. Wang, S.S. Mangipudi, B.F. Canine, **A. Hatefi**, A designer biomimetic vector with a chimeric architecture for targeted gene transfer. *J Control Release* 137 (2009) 46-53.

Appendices

Appendix A: The Nanomedicine and Drug Delivery Symposium (2010) program highlights.

Appendix B: The published abstract for DOD IMPaCT 2011 conference.

Appendix C: Reference 1

Abstract#1847: DEVELOPMENT OF A NANOTECHNOLOGY PLATFORM FOR
PROSTATE CANCER GENE THERAPY

Arash Hatefi¹ and Yuhua Wang²

^{1,2}Rutgers, The State University of New Jersey, Piscataway, NJ

²Washington State University, Pullman, WA

Background and Objectives: The objective of this research was to develop a multifunctional vector that can condense therapeutic genes into nano-size carriers, target PC-3 prostate cancer cells specifically and transfect and kill them efficiently. To achieve the objective, we developed a vector composed of four repeating units of histone H2A, a fusogenic peptide, and a PC-3 specific targeting motif. The PC-3 cancer cell model was chosen as a target because it represents a subpopulation of metastatic cancer cells that do not overexpress human epidermal growth factor receptor 2 (HER2) making them non-responsive to treatment with anti-HER2 antibodies such as Herceptin. In addition, PC-3 cells don't overexpress coxsackie adenovirus receptor which makes it a poor candidate for adenoviral gene therapy. Therefore, there is a need for the development a vector that can fill this gap and used for the treatment of such cancer cells.

Methodologies: The vector was designed, genetically engineered in *Escherichia coli*, and purified using nickel column chromatography. The vector was complexed with pEGFP (encodes GFP) and pTK (encodes thymidine kinase) to form nanosize particles. The size of the nanoparticles was measured using dynamic light scattering technique by Malvern Nano ZS90 instrument. Vector/pEGFP complexes were used to transfect PC-3 (prostate cancer), RWPE-1 (normal prostate), and SKOV-3 (ovarian cancer) cells. The transfection efficiency was determined using flow cytometry. The vector-related cytotoxicity was also determined by a WST-1 cell toxicity assay. To evaluate the therapeutic efficacy, the vector was complexed with pTK and used to transfect PC-3 cells. Concurrently, PC-3 cells received 25uM of ganciclovir (prodrug) for a period of 7 days. The killing efficiency of vector/pTK complexes was determined by WST-1 cell toxicity assay.

Results: The results demonstrated that the vector is able to condense plasmid DNA into particles with sizes less than 100 nm, target PC-3 cancer cells but not RWPE-1 or SKOV-3 cells, and mediate efficient gene expression. The cell toxicity assay data also showed that the vector by itself does not have any detectable toxicity at its maximum efficiency. The in vitro therapeutic efficacy studies revealed that the vector is able to kill approximately 70% of the PC-3 cells only in the presence of ganciclovir.

Conclusions: Recombinant DNA technology has allowed us to create a targeted multifunctional vector that can specifically kill PC-3 prostate cancer cells with minimal impact on normal prostate cells.

Impact Statement: The proposed nanosystem has a significant impact on prostate cancer gene therapy because it could fill the gap where immunotherapy and adenoviral gene therapy are not effective in treating patients with metastatic prostate cancer.

nanomedicine and drug delivery symposium -

October 3 - 5, 2010

Omaha, Nebraska

NanoDDS'10

Omaha

Keynote Speakers

Joseph DeSimone (University of North Carolina at Chapel Hill)

Teruo Okano (Tokyo Women's Medical University)

Confirmed Speakers

Christine Allen (University of Toronto)

Mark Davis (California Institute of Technology)

Dennis Discher (University of Pennsylvania)

Iola Duarte (University of Aveiro)

Mohamed El-Sayed (University of Michigan)

Hamid Ghandehari (University of Utah)

Justin Hanes (The Johns Hopkins University)

Arash Hatefi (Washington State University)

W.E. Hennink (Utrecht University)

Leaf Huang (University of North Carolina at Chapel Hill)

Akihiro Kishimura (The University of Tokyo)

Philip S. Low (Purdue University)

Robert Luxenhofer (Dresden University of Technology)

Andrew Mackay (University of Southern California)

Muthiah Manoharan (Alynlam Pharmaceuticals)

Olivia Merkel (Philipps University, Marburg)

Xin Ming (University of North Carolina at Chapel Hill)

Tamara Minko (Rutgers University)

Randall Mrsny (University of Bath)

Vladimir Muzykantov (University of Pennsylvania)

Yukio Nagasaki (University of Tsukuba)

Derek O'Hagan (Novartis)

David Owen (Starpharma)

Robert Prud'homme (Princeton University)

Tom Redelmeier (Northern Lipids, Inc.)

Sonke Svenson (Cerulean Pharma Inc.)

Organizing Committee

Chair: Alexander Kabanov (University of Nebraska Medical Center)

Co-Chair: Tatiana Bronich (University of Nebraska Medical Center)

Christine Allen (University of Toronto)

Hamid Ghandehari (University of Utah)

Ralph Lipp (Eli Lilly & Company)

Christine Allmon (University of Nebraska Medical Center)

Marsha Fau (University of Nebraska Medical Center)

Keith Sutton (University of Nebraska Medical Center)

Registration and abstract submission: www.nanodds.org

**8th International Nanomedicine
and Drug Delivery Symposium
Omaha, NE, USA October 3-5, 2010**

The field of nanomedicine has seen an exponential growth in the level of activity, investment, and development in recent years as evidenced by the creation of new companies, the launch of new scientific journals such as *Nature Nanotechnology*, *Nano Letters*, and *Nanomedicine-UK*, the establishment of new programs and departments in universities and government research institutions, as well as an extraordinary increase in the number of nanomedicine-focused publications. Developments in nanomedicine have already achieved true improvements in human health with the great promise of even more to come. Drugs relying on delivery or formulation in nanotechnologies such as Doxil™ have been approved for human use while others like NK911, NK105, and SP1049C have entered clinical trial development. Imaging agents for disease detection, characterization and staging such as Fenestra™ have also reached the late stages of pre-clinical development. While nanomedicine now features prominently in many scientific meetings, conferences and symposia, the NanoDDS meeting series remains unique among them.

NanoDDS, now entering its eighth year, began in 2003 as a US-Japan mini-symposium organized by Dr. A. Kabanov and Dr. K. Kataoka. According to Dr. Ruth Duncan it was the first scientific meeting of its kind. NanoDDS has since established itself as an internationally-recognized, medium-sized and focused symposium highlighting new discoveries and developments in the field of nanomedicine while also serving as a forum to discuss the issues of pre-clinical and clinical development of nanomedicines. The intimate format of NanoDDS sets it apart from all other meetings of its kind, providing an excellent environment for interaction, networking, discussion, creativity and innovation between trainees (graduate students and post-doctoral fellows) and some of the world's leading academic scientists and industry specialists. These interdisciplinary interactions should aid in fostering new, fruitful collaborations, leap-step advances, and ground-breaking discoveries.

**SCIENTIFIC PROGRAM
Sunday October 3rd, 2010**

First Keynote Presentation

Molecular Design of Intelligent Surfaces for Drug and Cell Delivery - *Teruo Okano, Tokyo Women's Medical University, Japan*

Session 1: Nanomedicines in Cancer (Part One)
Image Guided Design of Liposome-Based Cancer Therapy - *Christine Allen, Univ. of Toronto, Canada*

Ligand-Targeted Molecules for Imaging and Therapy of Cancer and Inflammatory Diseases
Philip S. Low, Purdue University

Nanotechnology Strategies to Overcome Limitations in Drug Delivery: Opportunities and Challenges - *Tamara Minko, Rutgers University*

Session 2: Nanomedicines in Cancer (Part Two)
Nanoparticle Delivery of siRNA for Cancer Therapy
Leaf Huang, University of North Carolina-Chapel Hill

Architectural Influence of Nanocarriers on Tumor Distribution and Toxicity
Hamid Ghandehari, University of Utah

From Concept to Clinic with Targeted Nanoparticles Containing siRNA
Mark E. Davis, California Institute of Technology

Session 3: Clinical Translation of Nanomedicines
Industrial Session and Roundtable - From Bench to Bedside: *Tom Redelmeier of Northern Lipids Inc., David Owen of Starpharma, Derek O'Hagan of Novartis, Sonke Svenson of Cerulean Pharma Inc., Muthiah Manoharan of Alynlam Pharmaceuticals*

Monday October 4th, 2010

Second Keynote Presentation

Engineering Better Medicines and Vaccines - *Joseph DeSimone, University of North Carolina-Chapel Hill*

Session Four: Novel Nanoformulation Technologies
Facile Production of Nanoparticles for Difficult to Deliver Therapeutics: hydrophobic drugs, peptides, and siRNA - *Robert Prud'homme, Princeton Univ.*

Novel Nanoparticles Functionalized for Anti-Oxidative Stress
Yukio Nagasaki, University of Tsukuba, Japan

Polymersomes to Filomicelles - thickness, shape, flexibility, charge...

Dennis Discher, University of Pennsylvania

Thermosensitive Polymeric Micelles for Targeted Delivery - *W. Hennink, Utrecht Univ., Netherlands*

Session Five: Tackling Nanomaterial-Tissue Interfaces to Improve Therapies and Diagnostics
Nanocarriers for Antioxidants
Vladimir Muzykantov, University of Pennsylvania

Strategies to Enhance Nanoparticle Transcytosis
Randall Mrsny, University of Bath, United Kingdom

The Mucus Barrier to Viral and Non-Viral Gene Therapy - *Justin Hanes, Johns Hopkins University*

Poster Sessions and Oral Presentations

Tuesday October 5th, 2010

Session 6: Nanomedicine Research Reports
Following Dynamic Biological Processes through NMR Spectroscopy and Metabonomic Profiling
Iola Duarte, University of Aveiro, Portugal

Customization of Genetically Engineered Vectors for Targeted Gene Transfer to Different Cancer Cells - *Arash Hatefi, Washington State University*

Novel polymeric hollow capsules "PICsomes"
Akihiro Kishimura, University of Tokyo, Japan

Doubly-Amphiphilic Poly(2-oxazoline)s with Unusual Microenvironment as High-Capacity Drug Delivery Systems - *Robert Luxenhofer, Dresden University of Technology, Germany*

Genetically Engineered Polypeptosomes
J. Andrew Mackay, Univ. of Southern California

SPECT Imaging of in vivo siRNA Delivery
Olivia Merkel, Philipps Univ.-Marburg, Germany

Molecular and Quantitative Pharmacology of siRNA Oligonucleotides Delivered via Receptor-Mediated Endocytosis - *Xin Ming, University of North Carolina at Chapel Hill*

Design and Evaluation of "Smart" Degradable Particles for Effective Gene Silencing
Mohamed E.H. El-Sayed, University of Michigan

GENERAL INFORMATION

Symposium Location

The symposium will be held at the Hilton Omaha, Nebraska's only 4 diamond hotel, located at 1001 Cass Street and within easy walking distance of the Old Market, Nebraska's premiere arts and entertainment district. The Hilton Omaha is only a short drive from Omaha's airport, as well as many other attractions including the Holland Performing Arts Center, Joslyn Museum, Durham Western Heritage Museum, and the Henry Doorly Zoo.

Accommodations

Accommodations are available at the Hilton Omaha at reduced conference rates. Alternate accommodations may also be found at several nearby hotels. Please visit the symposium website www.nanodds.org for additional information.

Symposium Registration

To register for the symposium, or for additional information, please visit the symposium website www.nanodds.org. Fees are \$125 for graduate students and post-doctoral fellows, \$400 for academics, and \$1,200 for industry participants. These fees include admission to all three days of the symposium, an abstract book, name badge and conference packet, continental breakfasts, lunches, and refreshment breaks.

Call for Posters

The poster session will be the highlight of the symposium with time dedicated for poster viewing and discussion with the authors. A number of posters will be selected for oral presentations based on their scientific merit, innovation and clarity. Those interested in presenting their work during the poster session of the symposium should please visit www.nanodds.org for abstract submission guidelines and formats. Please email your abstract to nanodds@unmc.edu by Friday, August 27, 2010.

CONTACT

Questions about NanoDDS'10 may be directed to: nanodds@unmc.edu

www.nanodds.org



Contents lists available at ScienceDirect

Journal of Controlled Release

journal homepage: www.elsevier.com/locate/jconrel

A designer biomimetic vector with a chimeric architecture for targeted gene transfer

Yuhua Wang, Sriramchandra Sastry Mangipudi, Brenda F. Canine, Arash Hatefi*

Department of Pharmaceutical Sciences, Center for Integrated Biotechnology, Washington State University, P.O. Box 646534, Pullman, WA 99164, USA

ARTICLE INFO

Article history:

Received 11 November 2008

Accepted 8 March 2009

Available online 18 March 2009

Keywords:

Biomimetic vector

Non-viral vector

Designer biomacromolecule

Gene therapy

ABSTRACT

Designer biomimetic vectors are genetically engineered biomacromolecules that are designed to mimic viral characteristics in order to overcome the cellular barriers associated with the targeted gene transfer. The vector in this study was genetically engineered to contain at precise locations: a) four tandem repeating units of N-terminal domain of histone H2A to condense DNA into stable nanosize particles suitable for cellular uptake, b) a model targeting motif to target HER2 and enhance internalization of nanoparticles, and c) a pH-responsive synthetic fusogenic peptide to disrupt endosome membranes and promote escape of the nanoparticles into the cytosol. The results demonstrate that a fully functional, multi-domain, designer vector can be engineered to target cells with high specificity, overcome the biological barriers associated with targeted gene transfer, and mediate efficient gene transfer.

Published by Elsevier B.V.

1. Introduction

In recent years, scientific interest in nature, particularly in the field of life sciences, has grown tremendously. The science of biomimetics has the potential to advance many areas of technology including vector development for gene therapy research. Biomimetic vectors are designed to mimic the viral characteristics and perform an array of self-guided functions in order to overcome the cellular barriers. For administered therapeutic genes to successfully reach the nucleus of the target cells, a carrier (vector) should be designed to overcome cellular barriers. Accordingly, the carrier should be able to: a) condense DNA from a large micro-meter scale to a smaller nano-meter scale suitable for endocytic uptake and protection from nuclease degradation, b) be recognized by specific receptors on the target cells and internalize, c) promote the escape of the gene from the endosomal compartment into the cytosol, and d) assist the translocation of DNA from the cytosol to the nucleus [1].

While lipoplexes provide high transfection efficiency, their reproducibility and cytotoxicity remain a major concern [2]. On the other hand, cationic polyplexes are robust and relatively biocompatible but they suffer from poor gene-transfer efficiency [1]. Polymeric carriers for targeted gene transfer are generally synthesized using chemical synthetic methods. This results in the production of polymers with random sequences, distribution of molecular weights, and a limited ability to attach functional motifs at precise locations [3]. Consequently, the main limiting factor in polymeric gene delivery remains the establishment of a systematic correlation between polymer structure and gene transfection. In contrast to synthetic methods, genetic engineering techniques allow biosynthesis of limitless combinations of biomimetic motifs where there

is full control over the vector architecture, the sequence and length at a molecular level. As a result, the relationship between vector structure and gene transfer efficiency can be recognized both at the molecular and nano-scale. A novel technique has previously been reported by Ghandehari's group to genetically engineer and express highly cationic biopolymers with tandem repeating units in *E. coli* expression system [4]. Development of this technology provided the basic tools for the design and development of more complex non-viral gene delivery systems, namely Designer Biomimetic Vectors (DBVs). Herein, we report a vector which is an ensemble of molecules of biological and synthetic origins for targeted gene transfer.

We hypothesize that a DBV with chimeric architecture can be developed to target model cancer cells, mimic viral characteristics to break through intracellular barriers, and mediate efficient gene transfer. The major challenge to this approach is to preserve the functionality of each motif in the vector structure because one domain could interfere with the other and render the vector ineffective. To test the hypothesis, a vector was genetically engineered to contain at precise locations: i) four tandem repeating units of N-terminal domain of histone H2A peptide (4HP), ii) a synthetic single chain HER2 targeting motif (TM), iii) a fusogenic peptide (FP) named GALA [5], and iv) a cathepsin D substrate (CS) (Fig. 1). The positioning of a cathepsin D cleavage site in between 4HP and TM allows for dissociation of the targeting motif from the vector inside the endosomes where cathepsin D is abundant [6].

2. Materials and methods

2.1. Cloning and expression of the targeted vector

The gene encoding 4HP-CS-TM was designed; expression optimized, and synthesized by Integrated DNA Technologies (San Diego, CA) with N-terminal NdeI and C-terminal HindIII restriction sites. The

* Corresponding author. Tel.: +1 509 335 6253; fax: +1 509 335 5902.
E-mail address: ahatefi@wsu.edu (A. Hatefi).

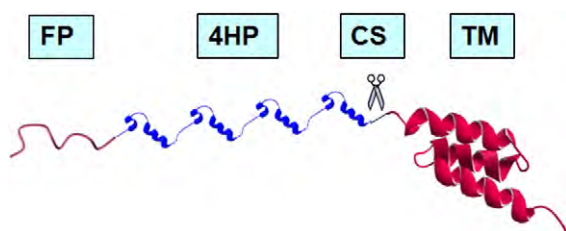


Fig. 1. Schematic representation of the multi-domain biomimetic vector. The vector is composed of a fusogenic peptide (FP), four tandem repeating units of histone H2A (4HP), a cathepsin D substrate (CS), and a HER2 targeting motif (TM). The 3D structures of the histone H2A and TM are predicted using SWISS-MODEL program.

synthesized gene was double digested with NdeI and HindIII (New England Biolabs, Ipswich, MA) restriction enzymes and cloned into a pET28b expression vector to make pET28b:4HP-CS-TM. The parent pET28b vector was purchased from EMD Biosciences (Gibbstown, NJ). The successful cloning of the 4HP-CS-TM gene in pET28b vector was verified by DNA sequencing. Subsequently, the fusogenic peptide gene (GALA) was synthesized by Integrated DNA Technologies with N-terminal NcoI and C-terminal NdeI restriction sites and cloned into pET28b:4HP-CS-TM expression vector to make pET28b:FP-4HP-CS-TM. The expression vector was transformed into *E. coli* BL21(DE3) pLysS (Novagen, San Diego, CA), grown using Barnstead-Labline MAX Q 4000 shaking incubator, and expressed by the addition of IPTG to a final concentration of 0.4 mM at 30 °C. Cells were collected, lysed, and centrifuged for 40 min at 30,000 *g* (4 °C) to pellet the insoluble fraction. The soluble fraction was recovered and loaded onto a Ni-NTA column (Amersham Biosciences, Piscataway, NJ) for purification. The column was washed with 40 volumes of wash buffer containing 100 mM NaH₂PO₄ (pH = 8), 10 mM Tris, 6 M GnHCl, and 20 mM imidazole and eluted with buffer containing 100 mM NaH₂PO₄, 10 mM Tris, 4 M GnHCl, and 250 mM imidazole. The purity of the vector was confirmed by loading 10 µg of DBV onto SDS-PAGE. The 66 kDa bovine serum albumin (BSA) with ca. 96% purity (Sigma) was used as control. The expression of the DBV was confirmed by western blot analysis (1 µg loading) using mouse monoclonal anti-6XHis. The amino acid content of DBV was analyzed by Commonwealth Biotechnologies Inc. (Richmond, VA). The purified vector was stored at –20 °C after addition of 50% glycerin. The exact molecular weight of the purified FP-4HP-CS-TM (DBV) was determined by mass spectroscopy at Washington State University mass spectroscopy core facility. Using the same protocol, 4HP-CS-TM which lacks fusogenic peptide (DBV/GALA) was expressed and purified.

2.2. Preparation of DBV stock solution

Before use, DBV was precipitated out of the storage buffer (50 mM NaH₂PO₄, 10 mM Tris, 4 M GnHCl, 250 mM imidazole, and 50% glycerin) by adding saturated ammonium sulfate solution (4.1 M) in small increments while incubating on ice. The salted out vector was collected in a microfuge tube by centrifugation at 5000 *g* and removal of supernatant. Subsequently, DBV was re-dissolved in 5 mM acetate buffer pH 3.5 to make ca. 2.0 mg/ml stock solution. This stock solution was used in ensuing studies.

2.3. Hemolysis assay

The pH activated membrane lysis of GALA was determined by hemolysis assay. Thoroughly washed sheep red blood cells were purchased from Innovative Research (Novi, MI) and constituted to 10⁸ cells/1 ml and supplemented with different amounts of vectors. The assays were performed in phosphate buffered saline (PBS) pH 7.4 and 5.5. After mild shaking and incubation for 1 h at 37 °C, the absorbance of lysate was measured at 541 nm. One percent Triton X-100 was used as a positive control whereas PBS (pH 7.4 and 5.5) was used as

negative control. DBV without GALA (DBV/GALA) at pH 5.5 was used as vector control. The data is reported as mean ± s.d., (*n* = 3). The statistical significance was evaluated using *t*-tests (*p* < 0.05).

2.4. Recognition of cathepsin D substrate by cathepsin D enzyme

Cathepsin D was purchased from Calbiochem (Gibbstown, NJ) and diluted to 6 nM with 50 mM Glycine-HCl buffer and 0.01% Triton X-100 as per manufacturer's protocol. Fifteen µg of vector was incubated with 2 units of Cathepsin D at 37 °C for 2, 4, and 18 h. The enzymatic reaction was stopped by adding SDS-PAGE sample loading buffer and boiling for 5 min at 95 °C. Samples were loaded on 15% Tris-glycine SDS-PAGE gels and visualized by coomassie staining.

2.5. Particle size, charge, and stability analysis

The mean hydrodynamic particle size and charge measurements for vector/pDNA complexes were performed using Dynamic Light Scattering and Laser Doppler Velocimetry respectively using Malvern Nano ZS90 instrument and DTS software (Malvern Instruments, UK). Various amounts of vector in 5 mM acetate buffer (pH 3.5) were added to 1 µg of pDNA (pEGFP) to form complexes at different N:P ratios (2 to 10) in a total volume of 100 µl deionized water. For example, to prepare N:P ratio of 10, 14 µg of vector was used to complex with 1 µg of pEGFP. After 15 min of incubation, the size and zeta potential of the complexes were measured and reported as mean ± SEM, (*n* = 3). Each mean is the average of 15 measurements and *n* represents the number of separate batches prepared for the measurements.

The stability of vector/pDNA nanoparticles (N:P 10) was studied at various pH conditions using a Malvern Nano ZS90 equipped with an automated titrator and the provided DTS software. For pH titrations, NaOH (0.1 and 0.5 M) and HCl (0.1 M) were used and the measurements were performed in triplicate.

2.6. Serum stability study

The neutralization of pDNA negative charges by DBV was examined using gel retardation assay in the absence of serum. One microgram pDNA (pEGFP, Clontech, CA, USA) was complexed with the DBV at N:P ratio of 10, incubated at room temperature for 15 min, and the mobility of pDNA was visualized on an agarose gel by ethidium bromide staining. To examine the effect of serum on the stability of particles, fetal bovine serum (Invitrogen, CA, USA) was added to the complexes at a final concentration of 10% (v/v) and incubated for 30 min at 37 °C. The complexes were then electrophoresed on a 1% agarose gel and pDNA mobility was visualized by ethidium bromide (Sigma, Milwaukee, WI) staining.

To evaluate the ability of the vector in protecting pDNA from endonucleases, complexes were formed in a microfuge tube and incubated with serum for 30 min. Subsequently, sodium lauryl sulfate was added (10%) to the tubes to decomplex pDNA from the vector. The released pDNA was electrophoresed on agarose gel and visualized by ethidium bromide staining.

2.7. Cell culture and transgene expression

SK-OV-3, MDA-MB-231, and NIH3T3 cells were seeded in 96-well plates at 4 × 10⁴ cells/well and incubated over night at 37 °C. Cells were transfected with vector/pEGFP complexes at various N:P ratios (equivalent of 1 µg pEGFP) in media supplemented with insulin, transferrin, selenium, ovalbumin, dexamethasone, and fibronectin. After 4 h, the media was removed and replaced with fresh media supplemented with 10% serum. When used, 100 µM chloroquine or 100 nM bafilomycin A1 (Sigma, Milwaukee, WI) was added to the media at the time of transfection. When applicable, 10 µM nocodazole (Sigma, Milwaukee, WI) was added 1 h prior to transfection to

depolymerize microtubules. The green fluorescent protein (GFP) was visualized after 48 h using an epifluorescent microscope (Zeiss Axio Observer Z1) to evaluate gene expression. Lipofectamine 2000 (Invitrogen) was used as a positive control to validate the transfection process of all the cell lines used in this study. DBV without GALA (DBV/GALA) was used as a control to examine the role of GALA in the vector structure. To quantify transfection efficiency, total green fluorescence intensity and percent transfected cells were measured using a flowcytometer (FacsCalibur, Becton Dickinson, San Jose, CA). The total fluorescence intensity of positive cells was normalized against the total fluorescence intensity of untransfected cells (background control). The total fluorescence intensity of cells transfected in the presence of drugs was normalized against the total fluorescence intensity of untransfected cells plus drugs. The data are presented as mean \pm s.d., $n = 3$. The statistical significance was tested using *t*-test ($p < 0.05$).

2.8. Inhibition assay

SK-OV-3 cells were seeded in 96 well tissue culture plates at 4×10^4 cells/well in 200 μ l McCoy media supplemented with 10% serum. After overnight incubation, cells were washed and incubated in serum free media for 4 h. A serial dilution of targeting peptide was prepared (0, 0.035, and 1.2 nM) and added to the cells followed by the addition of vector/pEGFP complexes (N:P 10). Cells were then incubated at 37 °C for 2 h followed by replacing the media supplemented with 10% serum. The expression of green fluorescent protein was measured by flowcytometry. The data are reported as mean \pm s.d., $n = 3$. The statistical significance was determined using *t*-test ($p < 0.05$).

2.9. Cell viability assay

SK-OV-3 cells were seeded in 96-well plates at 4×10^4 cells/well in McCoy media supplemented with 10% serum and incubated overnight. Cells were treated with serial dilutions of vector or vector/pEGFP complexes for 2 h. The media was removed and replaced with fresh McCoy media supplemented with 10% serum followed by overnight incubation at 37 °C humidified CO₂ atmosphere. The control well received PBS only. The next day WST-1 reagent (Roche Applied Science, Indianapolis, IN) was added, incubated for 4 h, and absorbance was measured at 440 nm. The measured absorbance for test groups is expressed as percent of the control where the control is defined as %100 viable. The data are reported as mean \pm s.d., $n = 3$. The statistical significance was evaluated using a *t*-test ($p < 0.05$).

The morphology of the SK-OV-3, MDA-MB-231 and NIH3T3 cells before and after transfection was examined by an inverted light microscope.

3. Results

3.1. Cloning, expression and identification of DBV

Using the cloning strategy shown in Fig. 2a, the DBV gene was cloned into pET28b and the fidelity of the sequence to the original design was confirmed by DNA sequencing. The DBV was expressed in *E. coli* and purified under stringent conditions with a 5 mg/l yield using affinity chromatography (Fig. 2b). The purity of the DBV in comparison to BSA (Fig. 2b, lane 2) is estimated to be above 96%. We have previously demonstrated that highly cationic vectors can be expressed in *E. coli* under similar conditions [4,7]. The exact molecular weight of the DBV was also determined by mass spectroscopy (MALDI-TOF) to be 28,522 Da (Fig. 2c). The result of amino acid content analysis demonstrated that in general the theoretical and experimental values are in close agreement (supplementary Table 1).

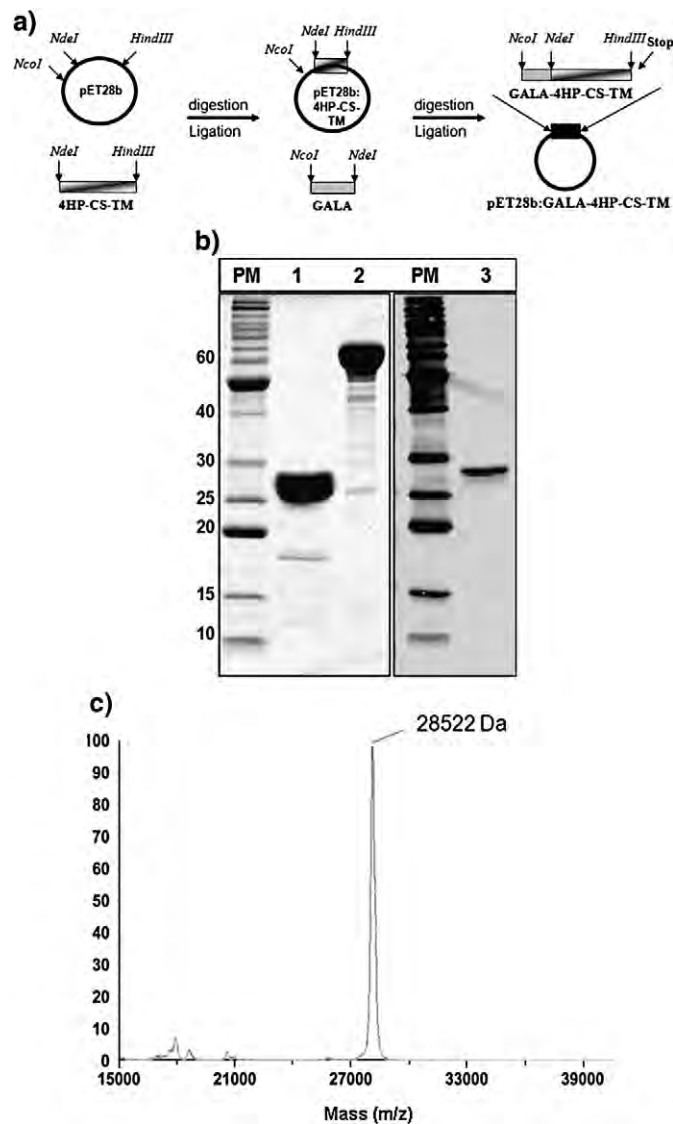


Fig. 2. Cloning, expression, and characterization of the purified targeted vector. a) An overview of the cloning strategy used to clone GALA-4HP-CS-TM gene into pET28b expression vector. b) SDS-PAGE (left panel) of the purified DBV (GALA-4HP-CS-TM). PM stands for protein marker; Lane 1 is purified DBV and lane 2 is BSA with ca. 96% purity. Lane 3 is the expressed DBV identified by western blot analysis (right panel). c) The MALDI-TOF picture of the purified DBV. The molecular weight was determined to be 28,522 Da.

3.2. Hemolytic assay

The ability of the DBV to lyse the membranes at low pH was examined by incubating the red blood cells with the vector at two different concentrations and pH conditions. In comparison to negative control group (buffer only), the results revealed that the vector was lytic only in acidic environment (pH 5.5). No significant cell lysis was observed at pH 7.4 or with the DBV/GALA at pH 5.5 (Fig. 3a). In addition, no significant difference in hemolytic activity of DBV between 1 and 10 μ g concentrations was observed.

3.3. Recognition of cathepsin D substrate by cathepsin D enzyme

The availability of the cathepsin D substrate to the protease was examined by incubating the DBV with cathepsin D enzyme. The molecular weight of the undigested DBV (FP-4HP-CS-TM) is 28.5 kDa (Fig. 3b, lane 2) whereas the molecular weights of the digested byproducts (i.e., FP-4HP and TM) are estimated to be approximately

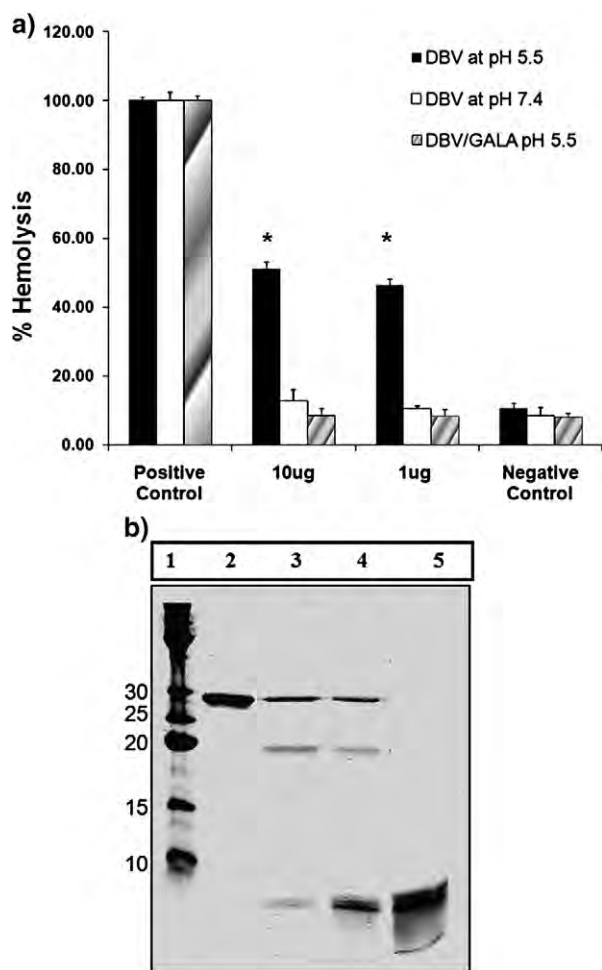


Fig. 3. Biological characterization of the targeted vector. a) Hemolysis assay for DBV at two different pH (5.5 and 7.4) and vector concentrations (1 and 10 μ g). Triton X-100 was used as positive control and PBS (pH 5.5 and 7.4) as negative controls. DBV without GALA (DBV/GALA) at pH 5.5 was also used as vector control (hatched bar). b) Digestion of targeted vector with cathepsin D protease. Lane 1 is the protein marker, lane 2 is the undigested targeted vector (28.5 kDa), lane 3 is digested vector by cathepsin D after 2 h resulting in one band at 21.5 kDa and one band at ca. 7 kDa, lane 4 is the digested vector after 4 h, and lane 5 is the digested vector after 18 h.

21.5 and 7 kDa, respectively (Fig. 3b, lanes 3–5). The results show that after 2 h of incubation the vector is partially digested and as the incubation time increased the concentration of byproducts increased. After 18 h of incubation, cathepsin D enzyme non-specifically digested the band at 21.5 kDa resulting in the byproducts with molecular weights less than 7 kDa.

3.4. Particle size, charge, and stability analysis

The size and charge of the nanoparticles was examined at different N:P (positively charged nitrogen to negatively charged phosphate) ratios. It was observed that nanoparticles with sizes below 100 nm can be obtained. For example, at N:P ratio of 10, the pDNA was condensed into nanoparticles with 89 ± 4.5 nm size and $+22 \pm 5$ mV surface charge (Fig. 4a). The serum stability of the nanoparticles was visualized by agarose gel mobility assay. It was shown that the condensed pEGFP in these nanoparticles was fully neutralized and stable in the presence of 10% serum (Fig. 4b, lanes 2 and 3). Furthermore, while DBV was able to effectively protect pEGFP from degradation by the serum nucleases (Fig. 4b, lane 4), the uncondensed pEGFP was susceptible to degradation by the endonucleases (Fig. 4b, lane 5). The stability of the nanoparticles formed at N:P 10 was also studied in a broad pH range. These particles

demonstrated stability in a pH range of 4 to 9, but started to lose integrity at pH 10 or higher (Fig. 4c).

3.5. Identification of optimum N:P ratio for cell transfection

SK-OV-3 cells were transfected with the vector/pEGFP complexes at various N:P ratios to identify the optimum ratio for transfection. While gene transfer at all N:P ratios were observed, the highest level of transfection efficiency was observed among N:P ratios of 8 to 12

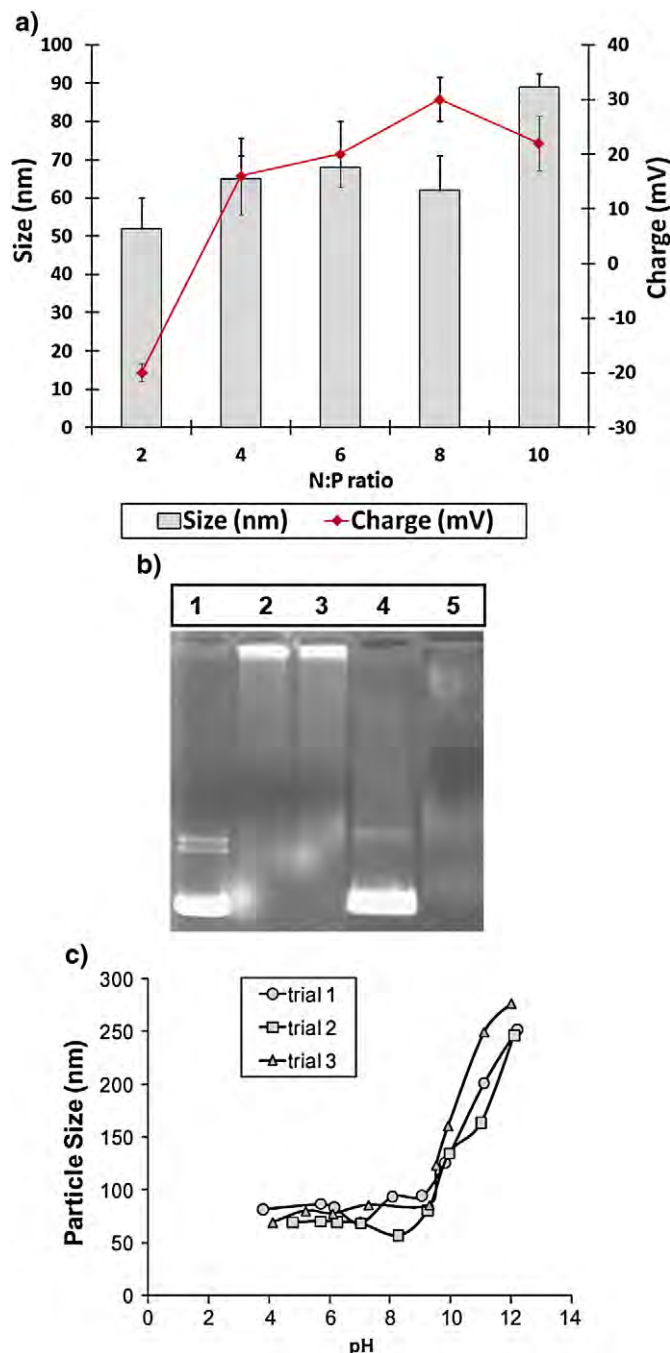


Fig. 4. Particle size, charge, and stability analysis. a) The particle size and charge analysis of vector/pEGFP complexes at various N:P ratios by dynamic light scattering. b) Gel mobility assay of pEGFP and vector/pEGFP complexes (N:P 10). Lane 1: pEGFP in the absence of serum. Lane 2: vector/pEGFP complexes (N:P 10) in the absence of serum. Lane 3: vector/pEGFP complexes (N:P 10) incubated with serum for 30 min. Lane 4: released pEGFP from the vector/pDNA complexes after incubation with serum for 30 min. Lane 5: pEGFP incubated with serum for 30 min. c) Particle stability analysis at various pH for vector/pEGFP complexes formed at N:P ratio of 10.

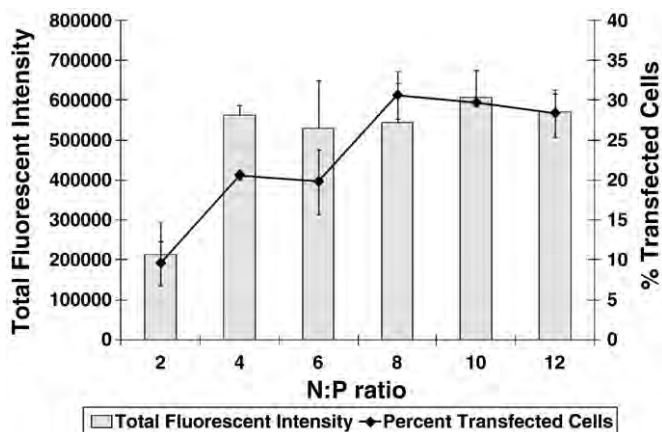


Fig. 5. Percent transfected cells as well as total green fluorescent protein expression for the SK-OV-3 cells transfected with vector/pEGFP complexes.

(Fig. 5). For example, at the N:P ratio of 10, $30 \pm 4\%$ of cells were transfected. The total fluorescent intensity at the N:P ratio 10 is $607,000 \pm 68,200$ light units which is a measure of total GFP

expression. As a positive control we used lipofectamine to validate the transfection protocol. The results showed that $36 \pm 5\%$ of cells were transfected when lipofectamine/pEGFP was used.

3.6. HER2 targeted gene transfer

An inhibition assay was performed to demonstrate internalization of nanoparticles via HER2. The results of this assay revealed that as the concentration of the targeting peptide (competitive inhibitor) increased, the levels of gene expression decreased (Fig. 6a). When 1.2 nM of the competitive inhibitor was used, the total green

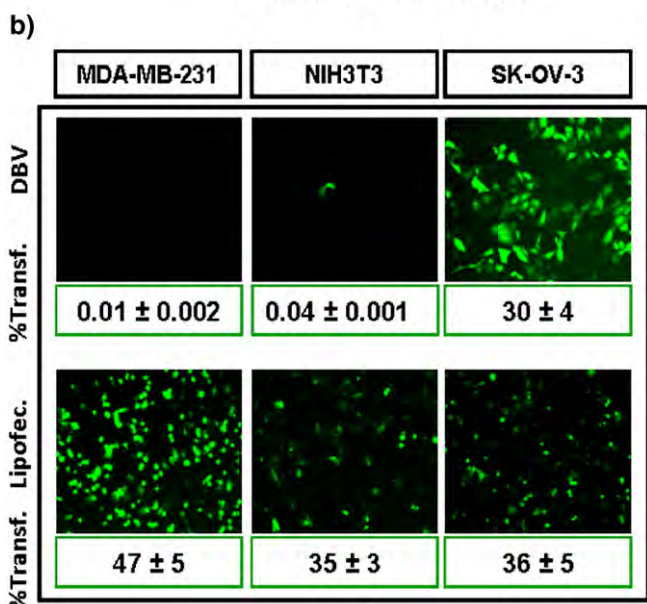
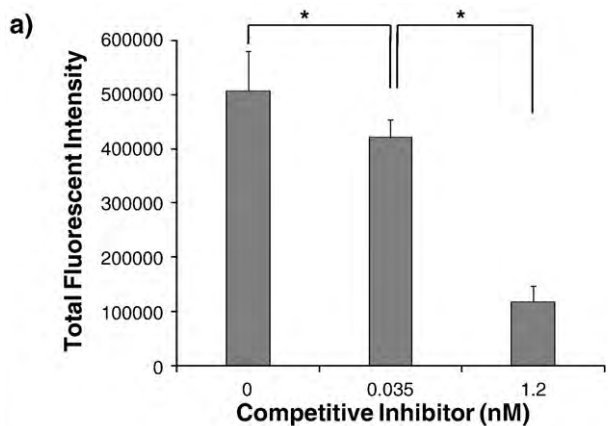


Fig. 6. Demonstration of HER2 targeted gene delivery. a) An inhibition assay to demonstrate the internalization of nanoparticles into the cells via HER2-mediated endocytosis. Targeting peptide at various concentrations was used as a competitor inhibitor. b) Qualitative and quantitative representation of the MDA-MB-231, NIH3T3 and SK-OV-3 cells transfected with vector/pEGFP complexes at N:P ratio of 10 and lipofectamine/pEGFP. The percentage of transfected cells is measured by flowcytometer.

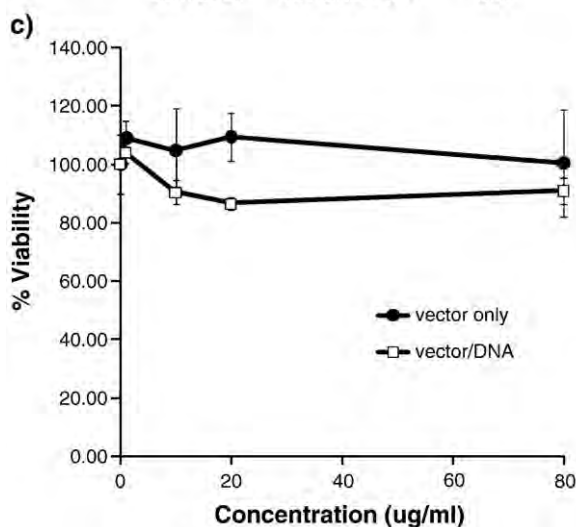
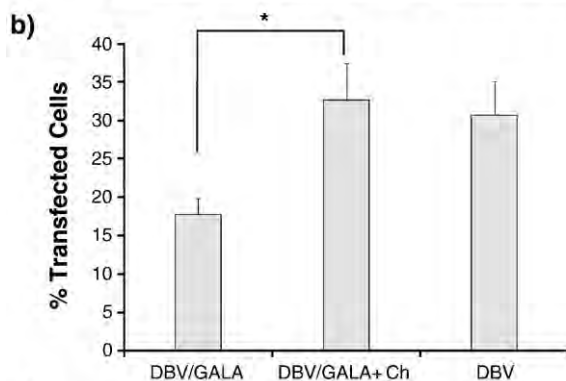
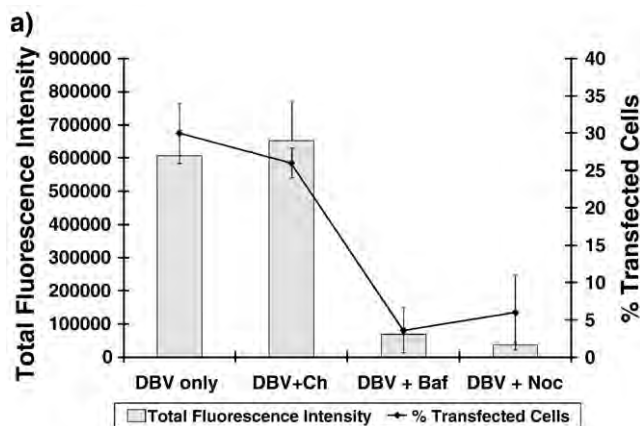


Fig. 7. a) Comparison of transfection efficiency among DBV, DBV in the presence of chloroquine (Ch), DBV in the presence of baflomycin A1 (Baf) and DBV in the presence of nocodazole (Noc). b) Comparison of percent transfected cells among DBV, DBV without GALA (DBV/GALA) and DBV without GALA plus chloroquine. c) WST-1 cell toxicity assay for SK-OV-3 cells. Cells were treated with various concentrations of vector or vector/pEGFP complexes ranging from 0 to 80 $\mu\text{g/ml}$ of vector.

fluorescent protein expression reduced from $507,000 \pm 73,000$ to $118,000 \pm 30,000$ light units. This is approximately 80% inhibition in gene expression.

HER2 targeted and cell selective gene transfer was examined by using vector/pEGFP complexes at N:P 10 to transfect HER2 positive SK-OV-3 (ovarian cancer) and HER2 negative MDA-MB-231 (breast cancer) and NIH3T3 (fibroblasts) cells. The results showed that $30 \pm 4\%$ of the SK-OV-3 cells were transfected, whereas the percent transfected cells was extremely low for both MDA-MB-231 and NIH3T3 cell lines ($<0.1\%$) (Fig. 6b). Lipofectamine was able to non-selectively transfect all cell lines with relatively high efficiency.

3.7. Overcoming the endosomal barrier and microtubule mediated gene transfer

To examine the effect of fusogenic peptide (GALA) on enhancing escape of cargo into cytosol, SK-OV-3 cells were transfected with DBV in the presence and absence of bafilomycin A1 (Baf) and chloroquine (Ch). In the absence and presence of bafilomycin A1 the percentage of transfected cells was significantly reduced from 30 ± 4 to 3.6 ± 3 , respectively (Fig. 7a). However, no significant difference between the transfection efficiency was observed in the absence or presence of chloroquine (Fig. 7a). In addition, when cells were transfected with DBV without GALA (DBV/GALA), a significant reduction in percent transfected cells from 30 ± 4 to 16 ± 3 was observed (Fig. 7b). No significant difference in terms of percent transfected cells was observed when SK-OV-3 cells were transfected with DBV or DBV/GALA plus chloroquine (Fig. 7b). To examine microtubule mediated transport of the nanoparticles towards the nucleus, SK-OV-3 cells were transfected in the absence and presence of nocodazole (Noc). The results illustrated significant reduction in percent transfected cells from 30 ± 4 to 6 ± 5 and total green fluorescent expression from $607,015 \pm 68,186$ to $38,550 \pm 5565$ (Fig. 7a).

3.8. Cell viability

The results of the WST-1 cell viability assay in SK-OV-3 cells exhibited no significant cell toxicity at a concentration of up to $80 \mu\text{g/ml}$ (Fig. 7c). The effect of vector/pEGFP complexes on cell viability was also evaluated qualitatively by monitoring the cells morphology. No signs of stress were observed in SK-OV-3, NIH3T3 or MDA-MB-231 cells before and after transfection with nanoparticles.

4. Discussion

The main objective of this research was to demonstrate the ability to package multiple motifs from different origins and diverse functions into one vector while preserving the functionality of each. Several experiments were conducted to evaluate the functionality of each motif in the vector structure in terms of efficient pDNA condensation, cell targeting, pH dependent endosome membrane disruption, translocation towards nucleus via microtubules and mediating gene transfer.

The gene encoding DBV was cloned (Fig. 2a) and expressed in *E. coli* and the results demonstrate successful expression and purification of the DBV to high purity (Fig. 2b). The mass spectroscopy result determined that the exact molecular weight of the DBV is in close agreement with the expected theoretical value of 28,561 Da (Fig. 2c). This confirms the expression of the DBV with exact length and sequence in a biological system. The vector was further characterized physicochemically and biologically to assess the functionality of each motif in the vector structure.

At the N-terminus of the vector structure, a synthetic pH-responsive pore-forming peptide (GALA) is designed to assist in escape of the cargo into cytosol [8]. Therefore, the pH responsiveness of the targeted vector in terms of lysing red blood cells under acidic pH

5.5 and physiologic pH 7.4 was evaluated. This feature of GALA is extremely important as it minimizes the possibility of causing cell damage while circulating in the blood stream. The results exhibits that the vector did not have hemolytic activity at pH 7.4, but was able to significantly lyse the red blood cells at pH 5.5 (Fig. 3a). This demonstrates that positioning of GALA at the vector's N-terminus preserves its amphipathic fusogenic functionality.

It was also mentioned that the engineered cathepsin D substrate in the vector structure is to facilitate dissociation of the targeting motif inside endosomes by cathepsin D enzyme. The vector was incubated with cathepsin D enzyme to evaluate the accessibility of the substrate to the enzyme. The results showed that the substrate was readily available to the protease (Fig. 3b, lane 2 and 3). This means that the dissociation of the targeting peptide from the vector can occur under *in vitro* conditions, but direct *in vivo* measurement of the kinetics of dissociation is not feasible at this point. Nevertheless, this observation suggests that the probability for the vector to shed the targeting motif inside endosomes exists. Because the targeting motif is designed to facilitate internalization of nanoparticles, its removal after receptor mediated endocytosis could result in better exposure of GALA on the nanoparticle surface facilitating interaction with the endosome membrane. In the next steps, we examined the ability of the DBV to condense pDNA into stable nanosize carriers, vector mediated gene transfer, and the effectiveness of TM in targeting cells over-expressing HER2.

While full length histone H1, H2, H3, and H4 have been used as gene transfer agents with limited success [9], we have utilized the N-terminal domain of histone H2A (residues 1–37) which is sufficient to condense plasmid DNA (pDNA) into particles suitable for cellular uptake [10]. However, one major problem associated with the use of short peptides is their limited capability to form stable nanosize particles with pDNA. It has been shown that peptides as short as 20 amino acids are able to condense pDNA into nanosize particles, but they fail to form stable nanoparticles under the complex physiological environment [11]. To overcome this hurdle, cationic peptides can be polymerized to enhance their affinity towards pDNA resulting in stable particles [7,12]. As a starting point, we designed four tandem repeating units of histone H2A in the vector structure and examined the ability of the vector to form stable nanocomplexes with pDNA. It was observed that at N:P ratios of 2 to 10, the pDNA was condensed into nanoparticles with less than 100 nm size with slight positive charge (Fig. 4a). Nanoparticles in this size range are shown to be suitable for receptor mediated endocytosis as they can fit into clathrin-coated vesicles [13].

The stability of the nanoparticles in the presence of serum and protection of pDNA from endonucleases were also investigated. It was observed that the pEGFP in these nanoparticles was fully neutralized, remained stable in the presence of 10% serum (Fig. 4b, lanes 2 and 3) and effectively protected pDNA from degradation by the serum nucleases (Fig. 4b, lane 4). These results suggest that the DBV effectively condensed pEGFP shielding it from serum endonucleases.

To observe the behavior and stability of nanoparticles under various pH conditions, the size of the nanoparticles was measured over titration of a broad pH range. This is an important measurement because these nanoparticles are expected to be exposed to not only pH 7.4 of cell cytoplasm but the low pH of endosomes. While these particles demonstrated stability in the pH range of 4 to 9, they started to lose integrity at pH 10 or higher (Fig. 4c). This was expected as lysine residues in the vector structure neutralize at pH values close to their pKa (i.e., 10.8) resulting in unstable nanoparticles. Stability of nanoparticles at pH 4.0 is an indication that they may survive the low pH environment of late endosomes. The stability of nanoparticles at this low pH could provide the opportunity for the fusogenic peptide (GALA) to more effectively interact with the endosome membranes and disrupt their integrity.

So far, we have demonstrated that the vector containing four repeating units of histone H2A is able to condense pDNA into stable

nanoparticles in the presence of serum and broad pH range. The next logical step is to evaluate the ability of the vector to mediate gene transfer. SK-OV-3 cells were transfected with the vector/pEGFP complexes at various N:P ratios to identify the optimum ratio for transfection studies. While the highest levels of transfection efficiency was observed at N:P ratios of 8 to 12 (Fig. 5), we chose to use N:P 10 in subsequent studies. As a positive control we used lipofectamine to validate the transfection protocol. It is of paramount importance to appreciate that non-targeted commercially available transfection reagents such as lipofectamine are usually formulated to flocculate into large size particles, in this case 645 ± 37 nm, so that they can precipitate readily onto the cells surface for maximum transfection efficiency. Such gene transfer reagents may not be suitable for systemic gene delivery not only due to their large particle size but non-specific binding to normal cells. For targeted nanoparticles, size below 200 nm is crucial in order to mediate efficient gene transfer because such nanoparticles need to fit into clathrin-coated vesicles for efficient receptor mediated endocytosis [13]. Consequently, higher rate of gene transfer for lipofectamine makes it a better gene transfer reagent for *in vitro* cell transfection studies but less effective vector for systemic gene therapy.

It has been demonstrated that presence of a targeting motif on the surface of nanoparticles significantly enhances their internalization into target cells [14]. In this study, as a model targeting motif, a single chain 57 amino acid affibody with high affinity towards HER2 (picomolar) was designed in the vector structure [15]. An inhibition assay was performed to demonstrate the functionality of the affibody on the surface of the nanoparticles and their internalization via HER2-mediated endocytosis. This was evaluated by pre-treatment of SK-OV-3 cells with the targeting peptide to saturate the receptors followed by transfection of the cells with vector/pEGFP complexes. The results of this assay revealed that as the concentration of the targeting peptide (competitive inhibitor) increased, the levels of gene expression decreased (Fig. 6a). This signifies that the nanoparticles were utilizing HER2 to enter the cells.

In addition, to examine the ability of the vector to target HER2 positive cells with high specificity, three well characterized cell lines (SK-OV-3, MDA-MB-231, and NIH3T3) were selected as a model to test this hypothesis. Orlova et al. [15], have previously demonstrated that the HER2 targeted affibody is able to selectively target SK-OV-3 ovarian cancer cells which over-express HER2. As negative controls we chose the breast cancer cell line MDA-MB-231 which has very low levels of HER2 expression [16] and NIH3T3 fibroblasts which over-expresses FGF2 receptors but not HER2. A similar approach by others has been employed to test the targetability of immunoliposomes [17,18]. To test the hypothesis, we used the vector/pEGFP complexes at N:P 10 and transfected MDA-MB-231 breast cancer and NIH3T3 fibroblast cells. The high level of transfection efficiency in SK-OV-3 cells versus extremely low levels in MDA-MB-231 and NIH3T3 can be attributed to the level of HER2 expression on the surface of cells (Fig. 6b). These results suggest that the presence of HER2 targeting motif in the vector structure facilitated internalization of particles in HER2 positive cells resulting in significant gene expression.

We then asked the question whether the presence of GALA in the vector structure had any effect on endosomal escape and transgene expression. GALA is expected to effectively increase the delivery of pDNA into the cytosol via membrane destabilization of acidic endocytotic vesicles containing vector/pDNA complexes. This was assessed by transfecting SK-OV-3 cells in the absence and presence of bafilomycin A1 and chloroquine. Chloroquine is a buffering agent known to disrupt the endosomal membrane by increasing the pH of the endosome environment and facilitating escape of the cargo into cytosol [19]. In contrast, bafilomycin A1 hampers the acidification of the endosome environment by inhibiting the vacuolar ATPase endosomal proton pump which significantly reduces the escape of the cargo into cytosol [20]. When SK-OV-3 cells were transfected in

the presence of bafilomycin, the transfection efficiency was significantly reduced highlighting the fact that the acidic pH of the endosomes is necessary for the escape of the nanoparticles into cytosol (Fig. 7a). This could be another reason to believe that the GALA motif in the vector structure became functional at low pH of endosomes. In addition, observing no significant increase in transfection efficiency in the presence of chloroquine implies that most of the internalized nanoparticles could escape into cytoplasm without remaining trapped inside the endosomes (Fig. 7a).

Furthermore, when SK-OV-3 cells were transfected with DBV without GALA (DBV/GALA), a significant reduction (ca. 50%) in transfection efficiency was observed in comparison to DBV (Fig. 7b). We expected to observe ca. 90% reduction in transfection efficiency close to the level of DBV in the presence of bafilomycin (i.e. 3.6 ± 3). This interesting observation could be attributed to the presence of histag (6 consecutive histidines) in the vector structure which may have disrupted endosome membranes due to the proton sponge effect [7,21]. Assuming that one pEGFP molecule is packaged in one nanoparticle, at N:P ratio of 10 approximately 9400 histidine residues exist. This could be an indication that to efficiently disrupt endosomes both fusogenic activity and proton sponge effect could be utilized simultaneously.

We also transfected cells with DBV/GALA in the presence of chloroquine to evaluate whether the observed 50% reduction in transfection efficiency was due to entrapment of nanoparticles inside the endosomes. The results elucidated that a significant subpopulation of the nanoparticles did remain trapped inside endosomes and could not escape into cytoplasm to mediate gene transfer (Fig. 7b). These results in combination with the results obtained from the hemolysis assay suggest that GALA played a significant role in enhancing gene expression due to its pH-dependent fusogenic activity.

To date, many effective non-viral gene delivery systems have been developed with the ability to overcome the barriers of gene delivery to the cytoplasm. However, studies have shown that the cellular uptake of plasmid DNA does not correlate with efficient cell transfection [22]. Although there is limited understanding of the cellular and molecular mechanisms involved with synthetic vector mediated gene transfer, transfection efficiency appears to be essentially limited by inefficient trafficking of DNA to the site of gene transcription in the nucleus [23]. Thus, an active translocation of pDNA from cytosol to the nucleus could reduce cytosolic residency time and minimize the possibility of pDNA degradation by the cytoplasm endonucleases. To examine whether the nanoparticles in this study utilized microtubules to reach nucleus, SK-OV-3 cells were transfected in the presence and absence of nocodazole, a reagent known to depolymerize microtubule structure [24,25]. The results revealed significant reduction in transfection efficiency when microtubule network was disrupted (Fig. 7a). Therefore, it can be deduced that the nanoparticles may have exploited microtubules to reach the nucleus. Histone H2A is shown to bear an inherent nuclear import signal in its structure which utilizes microtubules to be actively transported to the nucleus [10]. Therefore, presence of this signal sequence could have contributed to microtubule mediated transfer of the nanoparticles to the perinuclear membrane. Although it would be unlikely for the nanoparticles in this study with an average 89 nm particle size to go through the 30 nm diameter nuclear pore complex, it is highly likely that they enter the nucleoplasm during the mitosis phase when the nuclear membrane dissolves.

So far, we have examined each motif in the vector structure and showed that by correct positioning in the vector backbone, the functionality of each motif can be preserved. This can be explained by the fact that during the pDNA condensation process, hundreds of vector molecules participate to condense one molecule of pDNA. For example, at N:P ratio of 10, approximately 1570 vector molecules each containing 60 positively charged residues are employed to condense one pEGFP molecule (9462 negative charges). Therefore, it is probable to have a fraction of fully functional targeting motifs and FPs in the

vector/pDNA complex architecture. Thus, the nanocomplex is rendered ready to bind to the receptors, fuse with the endosome membranes, and utilize the microtubules for active translocation of genetic material to the cell nucleus.

To examine whether the vector/pEGFP complexes had any effect on the viability of the cells and in turn negatively affecting cell transfection efficiency, SK-OV-3 cells were incubated with the vector or vector in complex with pEGFP. The results exhibited no significant cell toxicity at a concentration of up to 80 µg/ml (Fig. 7c). This shows that the vector was not toxic and could not negatively impact transfection efficiency. In our transfection studies with MDA-MB-231 and NIH3T3 we did not observe any change in morphology or signs of stress which could be another indication that the vector is relatively non-toxic.

One last question that still remains unanswered is why all cells were not transfected since the vector seems to have overcome the major cellular barriers. Besides the dose of administered pEGFP, the answer could be due to the abundance of entry gates (i.e., HER2) on the surface of cancer cells which determines the number of particles that can be internalized. The relationship between the number of receptors on the cells surface and transfection efficiency has been demonstrated in adenoviruses which rely on coxsackie adenovirus receptor (CAR) to enter cells [26]. In addition, it is likely that not all SK-OV-3 cancer cells will over-express HER2 as cancer cell populations are usually heterogeneous. Nonetheless, other more complex explanations could be involved with this process which opens the door for more mechanistic studies to unravel the mysteries of efficient gene transfer. The results obtained from this study justify further evaluation of nanoparticles in terms of therapeutic efficacy, immunogenicity and toxicity in animal models.

5. Conclusion

We have successfully demonstrated that a multi-domain designer vector with complex chimeric architecture can retain individual functionality of components. This allows for the creation of efficient and targeted systems that can be fine-tuned for various gene delivery needs. Such systems can be modified, equipped with a variety of targeting motifs, and programmed to transfer genes to various cell types with applications in gene therapy for cancer, cardiovascular disease, cystic fibrosis and wound healing among others.

Acknowledgement

This work was funded in part by the American Cancer Society (ACS-IRG-77-003-26).

Appendix A. Supplementary data

Supplementary data associated with this article can be found, in the online version, at doi:10.1016/j.jintimp.2009.03.007.

References

- [1] D.W. Pack, A.S. Hoffman, S. Pun, P.S. Stayton, Design and development of polymers for gene delivery, *Nat. Rev. Drug Discov.* 4 (7) (2005) 581–593.
- [2] H. Lv, S. Zhang, B. Wang, S. Cui, J. Yan, Toxicity of cationic lipids and cationic polymers in gene delivery, *J. Control. Release* 114 (1) (2006) 100–109.
- [3] D.W. Urry, Physical chemistry of biological free energy transduction as demonstrated by elastic protein-based polymers, *J. Phys. Chem., B* 101 (51) (1997) 11007–11028.
- [4] A. Hatefi, Z. Megeed, H. Ghandehari, Recombinant polymer-protein fusion: a promising approach towards efficient and targeted gene delivery, *J. Gene Med.* 8 (4) (2006) 468–476.
- [5] W. Li, F. Nicol, F.C.J. Szoka, GALA: a designed synthetic pH-responsive amphipathic peptide with applications in drug and gene delivery, *Adv. Drug Deliv. Rev.* 56 (7) (2004) 967–985.
- [6] A.M. Haines, A.S. Irvine, A. Mountain, J. Charlesworth, N.A. Farrow, R.D. Husain, H. Hyde, H. Ketteringham, R.H. McDermott, A.F. Mulcahy, T.L. Mustoe, S.C. Reid, M. Rouquette, J.C. Shaw, D.R. Thatcher, J.H. Welsh, D.E. Williams, W. Zauner, R.O. Phillips, CL22 – a novel cationic peptide for efficient transfection of mammalian cells, *Gene Ther.* 8 (2) (2001) 99–110.
- [7] B.F. Canine, Y. Wang, A. Hatefi, Evaluation of the effect of vector architecture on DNA condensation and gene transfer efficiency, *J. Control. Release* 129 (2) (2008) 117–123.
- [8] R.A. Parente, L. Nadasdi, N.K. Subbarao, F.C.J. Szoka, Association of a pH-sensitive peptide with membrane vesicles: role of amino acid sequence, *Biochemistry* 29 (37) (1990) 8713–8719.
- [9] M. Kaouass, R. Beaulieu, D. Balicki, Histonefection: novel and potent non-viral gene delivery, *J. Control. Release* 113 (3) (2006) 245–254.
- [10] D. Balicki, C.D. Putnam, P.V. Scaria, E. Beutler, Structure and function correlation in histone H2A peptide-mediated gene transfer, *Proc. Natl. Acad. Sci. U. S. A.* 99 (11) (2002) 7467–7471.
- [11] D.L. McKenzie, W.T. Collard, K.G. Rice, Comparative gene transfer efficiency of low molecular weight polylysine DNA-condensing peptides, *J. Pept. Res.* 54 (4) (1999) 311–318.
- [12] D.L. McKenzie, E. Smiley, K.Y. Kwok, K.G. Rice, Low molecular weight disulfide cross-linking peptides as nonviral gene delivery carriers, *Bioconjug. Chem.* 11 (6) (2000) 901–909.
- [13] J. Rejman, V. Oberle, I.S. Zuhorn, D. Hoekstra, Size-dependent internalization of particles via the pathways of clathrin- and caveolae-mediated endocytosis, *Biochem. J.* 377 (Pt 1) (2004) 159–169.
- [14] D.B. Kirpotin, D.C. Drummond, Y. Shao, M.R. Shalaby, K. Hong, U.B. Nielsen, J.D. Marks, C.C. Benz, J.W. Park, Antibody targeting of long-circulating lipidic nanoparticles does not increase tumor localization but does increase internalization in animal models, *Cancer Res.* 66 (13) (2006) 6732–6740.
- [15] A. Orlova, M. Magnusson, T.L. Eriksson, M. Nilsson, B. Larsson, I. Hoiden-Guthenberg, C. Widstrom, J. Carlsson, V. Tolmachev, S. Stahl, F.Y. Nilsson, Tumor imaging using a picomolar affinity HER2 binding antibody molecule, *Cancer Res.* 66 (8) (2006) 4339–4348.
- [16] G.E. Konecny, M.D. Pegram, N. Venkatesan, R. Finn, G. Yang, M. Rahmeh, M. Untch, D.W. Rusnak, G. Spehar, R.J. Mullin, B.R. Keith, T.M. Gilmer, M. Berger, K.C. Podratz, D.J. Slamon, Activity of the dual kinase inhibitor lapatinib (GW572016) against HER-2-overexpressing and trastuzumab-treated breast cancer cells, *Cancer Res.* 66 (3) (2006) 1630–1639.
- [17] T. Yang, M.K. Choi, F.D. Cui, S.J. Lee, S.J. Chung, C.K. Shim, D.D. Kim, Antitumor effect of paclitaxel-loaded PEGylated immunoliposomes against human breast cancer cells, *Pharm. Res.* 24 (12) (2007) 2402–2411.
- [18] M.E. Hayes, D.C. Drummond, K. Hong, W.W. Zheng, V.A. Khorosheva, J.A. Cohen, O.N.T. C, J.W. Park, J.D. Marks, C.C. Benz, D.B. Kirpotin, Increased target specificity of anti-HER2 nanospheres by modification of surface charge and degree of PEGylation, *Mol. Pharmacol.* 3 (6) (2006) 726–736.
- [19] A.K. Salem, P.C. Searson, K.W. Leong, Multifunctional nanorods for gene delivery, *Nat. Matters* 2 (10) (2003) 668–671.
- [20] E.J. Bowman, A. Siebers, K. Altendorf, Bafilomycins: a class of inhibitors of membrane ATPases from microorganisms, animal cells, and plant cells, *Proc. Natl. Acad. Sci. U. S. A.* 85 (21) (1988) 7972–7976.
- [21] J.P. Behr, The proton sponge: a trick to enter cells the viruses did not exploit, *Chimica* 51 (1997) 34–36.
- [22] V. Escriou, M. Carriere, D. Scherman, P. Wils, NLS bioconjugates for targeting therapeutic genes to the nucleus, *Adv. Drug Deliv. Rev.* 55 (2) (2003) 295–306.
- [23] J. Suh, D. Wirtz, J. Hanes, Efficient active transport of gene nanocarriers to the cell nucleus, *Proc. Natl. Acad. Sci. U. S. A.* 100 (7) (2003) 3878–3882.
- [24] J. Suh, D. Wirtz, J. Hanes, Real-time intracellular transport of gene nanocarriers studied by multiple particle tracking, *Biotechnol. Prog.* 20 (2) (2004) 598–602.
- [25] H. Salman, A. Abu-Arish, S. Oliel, A. Loyter, J. Klafter, R. Granek, M. Elbaum, Nuclear localization signal peptides induce molecular delivery along microtubules, *Biophys. J.* 89 (3) (2005) 2134–2145.
- [26] D. Li, L. Duan, P. Freimuth, B.W.J. O'Malley, Variability of adenovirus receptor density influences gene transfer efficiency and therapeutic response in head and neck cancer, *Clin. Cancer Res.* 5 (12) (1999) 4175–4181.